

COMPARISON OF RANGE STACKING AND OMEGA-K ALGORITHMS IN SYNTHETIC APERTURE SONAR PROCESSING

Marcin Szczegielniak¹, Damian Szczegielniak²

University of Technology and Life Sciences,
Kaliskiego 7, Bydgoszcz 85-796 Poland
¹szczegielniakm@wp.pl, ²dszczeg@utp.edu.pl

Summary: Synthetic Aperture Sonar (SAS) processing is continuously developing into a direction of better, more effective and accurate algorithms. It is preferable to use algorithms which don't introduce additional errors because of a phase approximation or digital data interpolation. One of them is Range Stacking. The short analysis of this algorithm, emphasizing its advantages and disadvantages in comparison with another reconstruction algorithm called Omega-k, was carried out in the paper. The simulated raw SAS signals for the stripmap mode were the basis of the practical part of the comparison. The set of examined SAS images included some signals after the spatial filtering with the use of Polar Format Processing. The results of the numerical simulation are shown and discussed in this paper.

Keywords: synthetic aperture sonar, range stacking, omega-k, comparison

1. INTRODUCTION

A stripmap SAS system in the three-dimensional spatial (x,y,z) domain during the data acquisition is depicted in Fig. 1A. The SAS system sends successive sound pulses perpendicular to the direction of the travel (the broadside case). The positions of the platform (where pulses are transmitted and received) are evenly spaced. This is because a constant **Pulse Repetition Frequency (PRF)** as well as a constant platform speed are assumed. The platform position and system parameters determine the size and shape of the aperture footprint on seafloor's surface. This footprint is swept along-track as the platform moves along ping by ping, illuminating the swath, so that the response of a scatterer on the seafloor is included in more than single sonar echo. An appropriate coherent combining of the signal returns (by means of a SAS reconstruction algorithm) leads to the formation of synthetically enlarged antenna of the length $2L$ (Fig. 1B), what is equivalent to obtaining a high-resolution reflectivity map of an acoustic backscatter strength.

The assumed ‘stop and hop’ model (the sonar is stationary between transmitting and receiving signals) is not particularly valid in real conditions because of the relatively low sound speed in water (in comparison with the propagation of electromagnetic waves and thus SAR systems). However, it seems to be good enough to compare two different SAS reconstruction algorithms and gets more appropriate for SAS systems operating at short target ranges (Tab. 1). No motion errors influence is taken into account in this paper. In order to simplify later analysis it’s possible to define the new variable

$$r = \sqrt{y^2 + h^2} \quad (1)$$

where h is the altitude of the platform and y denotes the spatial coordinate according to Figure 1A. Thanks to this abbreviation the imaging scene can be represented by the two-dimensional spatial (x, r) domain. The synthetic aperture domain will be represented by the variable \mathbf{x}' in order to distinguish from the coordinate x . A signal transmitted by an antenna can be written as

$$p_{tr}(t) = p(t) \cdot \exp[i\omega_c t] \quad (2)$$

where $p(t)$ and ω_c denote **Linear Frequency Modulated (LFM)** signal and a carrier frequency respectively. After receiving and demodulation the echo signal from the scatterer located at (x, r) , assuming the lossless environment, we have

$$e(\mathbf{x}', t) = \sigma \cdot p \left(t - \frac{2\sqrt{(x - \mathbf{x}')^2 + r^2}}{c} \right) \exp \left[-i\omega_c \cdot \frac{2\sqrt{(x - \mathbf{x}')^2 + r^2}}{c} \right] \quad (3)$$

where c is the sound speed in water, σ represents unknown reflectivity coefficient and \mathbf{x}' is the position of the platform (synthetic aperture).

The examined Range Stacking and Omega-k belong to the same group of relatively modern reconstruction algorithms which are free of Fresnel approximation errors [2]. However, the Range Stacking algorithm does not require any interpolation and thus it does not suffer from the truncation errors. Either one is used in high-resolution imaging SAR or SAS systems as the reconstruction step in synthetic aperture processing.

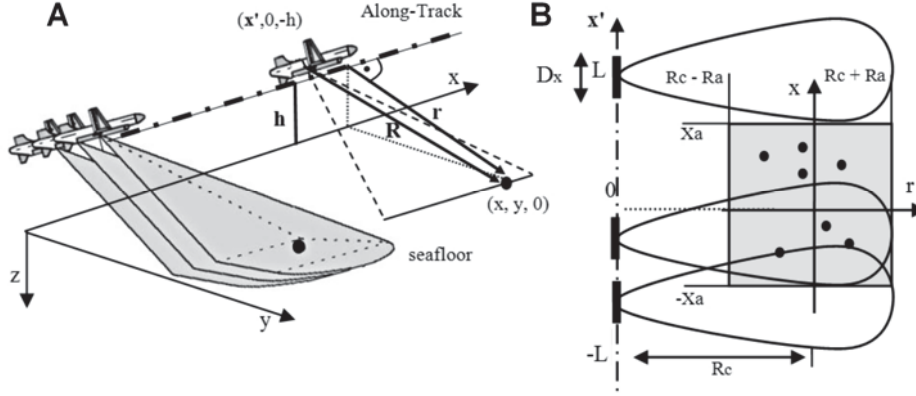


Fig. 1. Synthetic aperture imaging geometry: A) 3D; B) 2D

2. RANGE STACKING VS OMEGA-K

It is convenient to start with the mathematical model of the Omega-k algorithm and then go to the Range Stacking algorithm in order to show crucial differences. Taking advantage of the equation 3, we can write the SAS signal for the whole imaged area

$$e(\mathbf{x}', t) = \iint_{x r} \sigma(x, r) p \left(t - \frac{2\sqrt{(x - \mathbf{x}')^2 + r^2}}{c} \right) \exp \left[-i\omega_c \cdot \frac{2\sqrt{(x - \mathbf{x}')^2 + r^2}}{c} \right] dx dr \quad (4)$$

The aim of SAS processing is to determine the $\sigma(x, r)$ term which describes the desirable examined area reflectivity. Firstly, it's necessary to apply the Fourier transform on the raw SAS data. Using the simple rule $F_t[\delta(t - t_0)] = \exp(-i\omega \cdot t_0)$, where F_t is the forward Fourier transform with respect to time, we get SAS signal in the (\mathbf{x}', ω) domain

$$e(\mathbf{x}', \omega) = \iint_{x r} \sigma(x, r) \cdot P(\omega) \exp \left[-2i(\omega + \omega_c) \frac{\sqrt{r^2 + (x - \mathbf{x}')^2}}{c} \right] dx dr \quad (5)$$

$P(\omega)$ denotes the transformation of the transmitted sonar signal $p(t)$ defined in the equation (2). The next step is the transformation of this signal to the spatial frequency k_x domain by means of the Fourier transform with respect to the variable \mathbf{x}' in the form $F_{x'}[e(\mathbf{x}', \omega)]$. This problem can't be solved analytically. Fortunately, the above transform can be evaluated by means of the method of stationary phase in the following way

$$\begin{aligned}
F_{\mathbf{x}'} & \left[\exp \left(-2i(\omega + \omega_c) \frac{\sqrt{r^2 + (x - \mathbf{x}')^2}}{c} \right) \right] \approx \\
& \approx A \exp \left(-ir \sqrt{\left(\frac{2(\omega + \omega_c)}{c} \right)^2 - (k_{\mathbf{x}'})^2} - ik_{\mathbf{x}'} \cdot x \right)
\end{aligned} \tag{6}$$

where A is a slowly-fluctuating scaling term and therefore, it can be ignored. The above equation leads us eventually to the following integral which is the two-dimensional Fourier transform of the received SAS data

$$e(k_{\mathbf{x}'}, \omega) = \iint_{x r} \sigma(x, r) \cdot P(\omega) \exp[-ir \sqrt{\left(\frac{2(\omega + \omega_c)}{c} \right)^2 - (k_{\mathbf{x}'})^2} - ik_{\mathbf{x}'} \cdot x] dx dr \tag{7}$$

The Omega-k algorithm relies on the Stolt mapping defined below [1, 2]

$$k_r = \sqrt{\left(\frac{2(\omega + \omega_c)}{c} \right)^2 - (k_{\mathbf{x}'})^2} \tag{8}$$

$$k_x = k_{\mathbf{x}'} \tag{9}$$

After the mapping the expression (7) becomes

$$e(k_x, k_r) = \iint_{x r} \sigma(x, r) \cdot P(\omega) \exp[-ik_r \cdot r - ik_x \cdot x] dx dr \tag{10}$$

Spatial frequencies k_x and k_r represent the wavenumber in the along-track direction and the range direction respectively. Therefore, Omega-k is often called wavenumber algorithm. In order to complete the discrete inverse Fourier transform (the next step of this algorithm) the data must be evenly spaced in k_x and k_r domain. The nonlinear nature of the equation (8) causes unevenly spaced data. Therefore, it is required an interpolation to make possible a further processing. To sum up: the consequence of the Stolt mapping is the necessity of an interpolation of the SAS data. A target function estimating desirable $\sigma(x, r)$ function (the approximation results from a limited band of the SAS signal) is obtained from the equation (10) in the following way

$$f_c(x, r) = \iint_{k_x k_r} e(k_x, k_r) \cdot P^*(\omega) \exp[ik_r \cdot R_c] \cdot \exp[ik_r \cdot r + ik_x \cdot x] dk_x dk_r \tag{11}$$

where $P^*(\omega)$ is the complex conjugate of $P(\omega)$. The additional term which has appeared in the above equations allows to bring this signal to the low pass, i.e. this operation lets us to center the resultant SAS image at the reference distance

R_c . According to Fig. 1B, R_c and X_c represent the center of the illuminated area in the range and along-track domains respectively. The described case is broad-side type, where $X_c=0$. If it is not, we should introduce the additional function in the form $\exp(ik_x X_c)$.

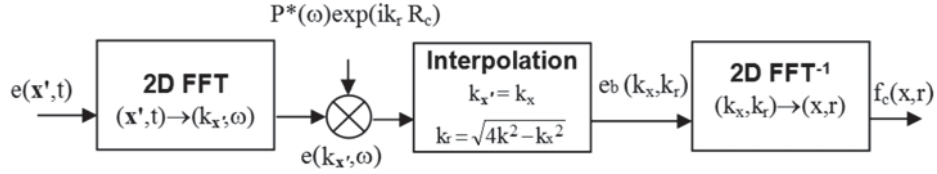


Fig. 2. Digital implementation of Omega-k algorithm

The Range Stacking algorithm allows to eliminate the Stolt mapping and thus an interpolation required in the Omega-k. The basic idea of this algorithm is the change of integral limits from (k_x, k_r) into $(k_{x'}, \omega)$ in the equation (11). It results in

$$f_c(x, r) = \iint_{k_{x'} \omega} e(k_{x'}, \omega) P^*(\omega) \exp[i\sqrt{4k^2 - (k_{x'})^2} \cdot R_c] \cdot \exp[i\sqrt{4k^2 - (k_{x'})^2} \cdot r + ik_{x'} \cdot x] \cdot J(k_{x'}, \omega) dk_{x'} d\omega, \quad (12)$$

$$\text{where } J(k_{x'}, \omega) = \frac{dk_r(\omega)}{d\omega} = \frac{4k}{c\sqrt{4k^2 - (k_{x'})^2}}$$

is the slowly fluctuating Jacobian function which results from the applied transformation. It can be ignored because its contribution in the reconstruction is negligible. We may assume as well that this term and the previous amplitude function A are absorbed in the signal $e(k_{x'}, \omega)$.

Let's introduce the auxiliary function, being the received echo signal in $(k_{x'}, \omega)$ domain from an ideal point target located at the distance $R_c + r_k$ and situated on the r -axis (Fig. 1B)

$$e_{r_k}(k_{x'}, \omega) = P(\omega) \cdot \exp\left(-i(R_c + r_k)\sqrt{4k^2 - (k_{x'})^2}\right) \quad (13)$$

Then, the equation (12) can be rewritten as follows

$$\begin{aligned}
f_c(x, r_k) &= \int_{k_{x'}} \left[\int_{\omega} e(k_{x'}, \omega) \cdot e_{r_k}^*(k_{x'}, \omega) d\omega \right] \cdot \exp(ik_{x'} \cdot x) dk_{x'} \\
&= \int_{k_{x'}} \left[\int_{\omega} e(k_{x'}, \omega) \cdot P^*(\omega) \exp\left(i(R_c + r_k) \sqrt{4k^2 - (k_{x'})^2}\right) d\omega \right] \cdot \exp(ik_{x'} \cdot x) dk_{x'}
\end{aligned} \tag{14}$$

In fact, the expression within square brackets is a matched filtering operation. The SAS signal is matched filtered with the reference function at the range r_k . Then, the outcome is integrated over the available fast-time frequencies ω to yield the marginal Fourier transform $F_c(k_{x'}, r_k)$. Applying the inverse Fourier transform with respect to $k_{x'}$, we get the target function $f_c(x, r_k)$ at the range r_k . The block diagram of the Range Stacking algorithm is depicted in Fig. 3. It is necessary to stress that shown steps have to be repeated for each range bin.

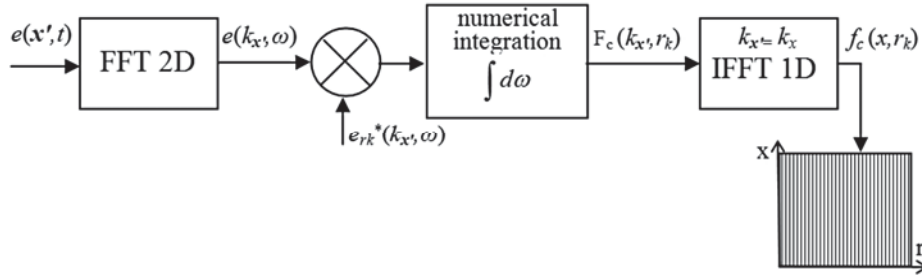


Fig. 3. Digital implementation of Range Stacking algorithm

3. COMPARISON CRITERIA

One possibility in order to specify a performance of a SAS system is to examine its impulse response. In such systems the impulse response can be obtained by measuring the system response to a single point target. As the result of the SAS reconstruction is two-dimensional image, quality parameters should be measured in two dimensions, azimuth and range. Because SAS impulse response is a sinc-like function, standard and well-known quantities such as **I**mpulse **R**esponse **W**idth (IRW), **P**eak **S**ideLobe **R**atio (PSLR), **I**ntegrated **S**ideLobe **R**atio (ISLR) were chosen as the quality parameters. The first one is the resolution measure and the others refer to contrast in a resultant image. In order to calculate the above parameters it is necessary to interpolate the SAS system impulse response firstly.

This is because a sinc-like function is represented by too few samples in a point target image (Fig. 4, the left image). The interpolation was carried out by centering the 32x32 window on the maximum of the main lobe and applying

zero padding in the frequency domain. The inverse Fourier transform IFFT with respect to the along-track and range directions gives the desirable image, appropriate to determine wanted parameters (Fig. 4, the right image). An additional comparison criterion was the difference graph of two normalized SAS images ($0 \leq \text{abs}[f_c(x,r)] \leq 1$) reconstructed by examined algorithms.

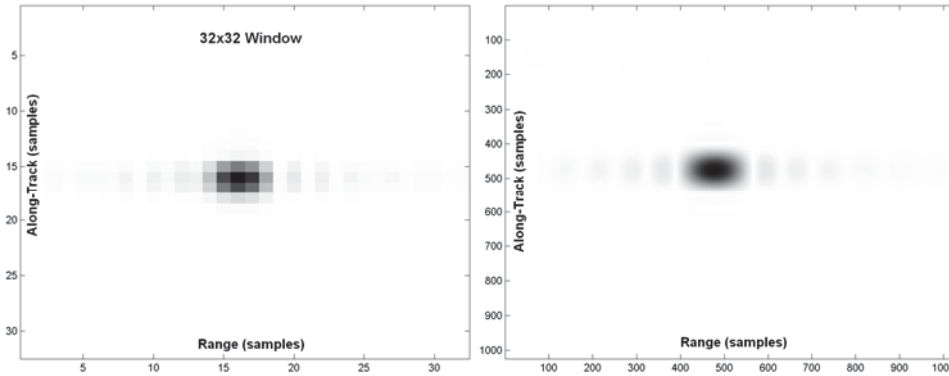


Fig. 4. SAS reconstruction of a point target: 32x32 window centered on the point target (left image); Interpolated point target (right image)

4. NUMERICAL SIMULATIONS

The assumed parameters of the stripmap SAS system are listed in Table 1. The raw SAS signals were generated for different point targets configurations in the imaged and simulated seafloor area. One of them is shown in Fig. 5A. The received SAS signals were next processed by the Omega-k and Range Stacking reconstruction algorithms to obtain high-resolution images of the illuminated area (Fig. 5B). Then, the 32x32 window was centered on each point target in the examined scene and parameters described in section 3 were calculated in order to compare the same point target processed by different reconstruction algorithms. Thanks to this it was possible to equate Omega-k to Range Stacking in following way

$$\delta = \frac{\text{Parameter_OmegaK} - \text{Parameter_RangeStacking}}{\text{Parameter_OmegaK}} * 100\% \quad (15)$$

Table 1. Assumed parameters of a stripmap SAS system

velocity of platform	0.5 [m/s]
c (sound speed in water)	1500 [m/s]
chirp bandwidth	5 [kHz]
chirp duration	5 [ms]
carrier frequency	100 [kHz]
PRF (Pulse Repetition Frequency)	15 [Hz]
D_x (sonar diameter in the along-track direction)	0.16 [m]
range resolution	0.0750 [m]
along-track resolution	0.0800 [m]
$2 * R_a$ (examined seafloor in the range direction)	20 [m]
$2 * X_a$ (examined seafloor in the azimuth direction)	10 [m]
R_c (distance to the center of the examined area)	30 [m]

The representative result of the comparison of two algorithms (for the SAS signal in figure 5A) is shown in Table 2. The main tool which allowed to emulate SAS system in the stripmap mode, to implement both algorithms, extract and prepare point target images, calculate suitable parameters and finally compare the obtained results was the Matlab environment.

Table 2. Relative differences δ (according to the equation 15) between parameters calculated for along-track and range profiles reconstructed by Omega-k and Range Stacking algorithms

Point Target	Along-Track Profile				Range Profile			
	PSLR	IRW 3 dB	IRW null-to-null	ISLR	PSLR	IRW 3 dB	IRW null-to-null	ISLR
1	-0.33	0	0	-0.24	0.27	0	0	0.15
2	0	0	0	0	0	0	0	0
3	0	0	0	0	0	0	0	0
4	0	0	0	0	0	0	0	0.02
5	0	0	0	0	0	0	0	0
6	0.03	0	0	0.04	-0.13	0	0	-0.38
7	0.39	0	0	0.33	0.18	0	0	-0.1
8	0.7	0	0	0.64	0.09	0	0	-0.05
9	0	0	0	0	0.04	0	0	0
10	0	0	0	0	0	0	0	0
11	0	0	0	0	0	0	0	0
12	0	0	0.66	-0.01	-0.04	0	0	0
13	-0.03	0	0	0	0	0	0	0
14	0	0	0	-0.03	0	0	0	0
15	0	0	0	-0.01	0	0	0	-0.03
16	0	0	0	0	0	0	0	0
17	0	0	0	0	0.04	0	0	0

Table 2 continued

18	0	0	0	0	0	0	0	0
19	0	0	0	0.01	0	0	0	0
20	-0.03	0	0	0.03	0	0	0	-0.03
21	0	0	0	0.01	0	0	0	0
22	0	0	0	0	0	0	0	0
23	0	0	0	0	0	0	0	0
24	-0.08	0	0	-0.06	0.04	0	0	0
25	0	0	0	0	0	0	0	0
26	0	0	0	-0.01	0	0	0	-0.03
27	0	0	0	0	0	0	0	-0.03
28	-0.03	0	0	-0.01	0	0	0	-0.03
29	0	0	0.65	-0.01	0	0	0	0.03
30	0	0	0	0.01	0	0	0	0
31	0	0	0	0	0	0	0	0
32	0	0	0	-0.03	0	0	0	0
33	0	0	0	0	0	0	0	0
34	0.03	0	0	0.03	0	0	0	-0.03
35	0	0	0	0.03	0	0	0	0
36	0	0	0	0	0	0	0	0
37	0.17	0	0.65	0.32	0.76	0	-1.14	0.73
38	-0.03	0	0	-0.01	0	0	0	0
39	0.39	0	-0.66	0.39	0.18	0	0	-0.1
40	0	0	0	0	0	0	0	0.03
41	0.03	0	0	0	-0.09	0	0	-0.23
42	0	0	0	0	0	0	0	0
43	-0.03	0	0	-0.08	-0.22	0	0	-0.33

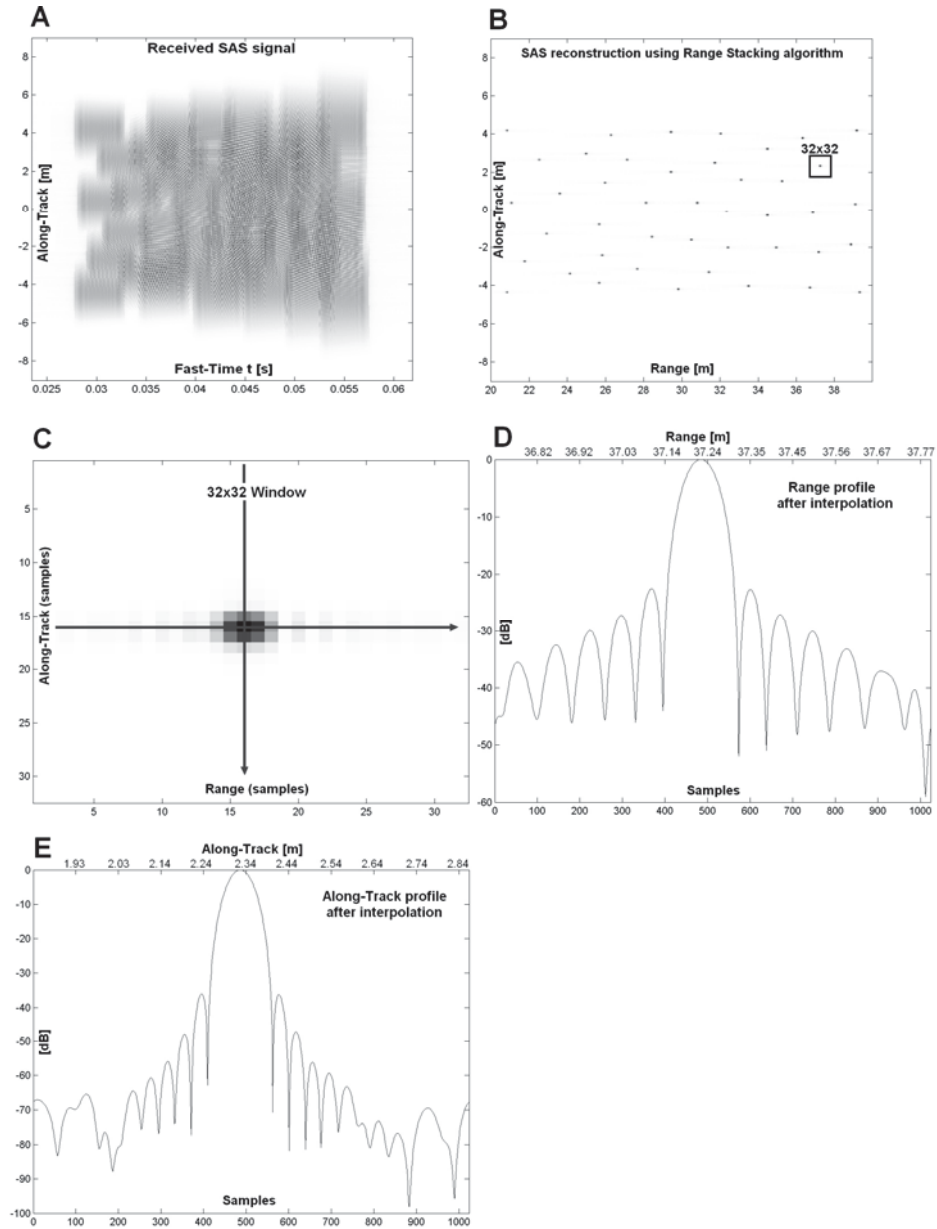


Fig. 5. Some results of the simulations: A) The Received raw SAS signal for 43 point targets; B) The resultant SAS image reconstructed by means of the Range Stacking algorithm; C) 32x32 window used to extract single point targets from the imaged scene; D, E) Range and along-track profiles retrieved by the Range Stacking processing and interpolated by zero padding in the frequency domain

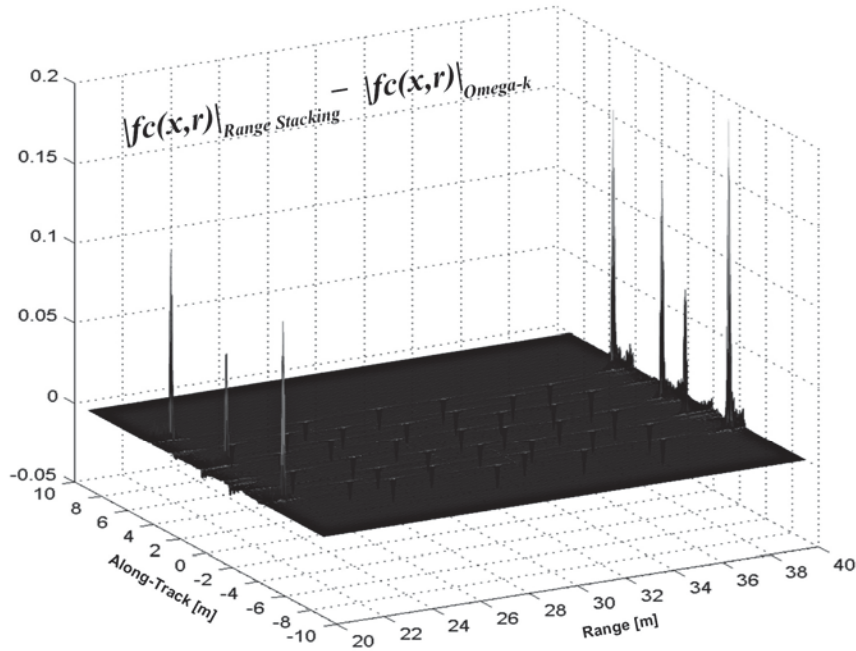


Fig. 6. Difference of two SAS images reconstructed by Range Stacking and Omega-k

5. SUMMARY AND CONCLUSIONS

More than a dozen SAS images containing points targets (randomly located in the illuminated scene) were examined. The square window was used to extract single point targets from reconstructed SAS images. The set of parameters (IRW, PSLR, ISLR) calculated on the basis of along-track and range profiles (Fig. 5D, 5E) of all point targets allowed to compare two different reconstruction algorithms, Range Stacking and Omega-k. The result of this comparison did not unambiguously indicate better algorithm. The examined relative differences δ were at very low level and did not exceed 2% (the maximum value for the SAS image in Figure 5A amounted to 1,13%). Despite occurring some differences, it seemed to be a little random because of appearing small positive and negative values in each column (e.g. Table 2) a comparable number of times. To recapitulate, it was difficult to note a clear trend here.

The opposite situation was with the interpretation of the difference graph of two normalized SAS images obtained by different reconstruction algorithms. As we can see in Figure 6, the biggest positive peaks (biggest differences) are at the edges of the graph. It means that these peaks in SAS images processed by Range Stacking algorithm have higher values what is undoubtedly its advantage. To be more precise, point targets on edges of the illuminated area are

better focused by the examined Range Stacking algorithm than Omega-k one. The graph in Figure 6 is a simple difference between two reconstructed SAS images $f_c(x,r)$ obtained by means of these two algorithms for exactly the same illuminated scene (point targets). This differential graph includes small negative peaks inside the area and bigger positive peaks at edges. Occurring small negative peaks are connected with the used normalization process ($0 \leq \text{abs}[f_c(x,r)] \leq 1$) of reconstructed SAS images (two different peaks were found as maximums and chosen for the normalization of two compared SAS images respectively). So, we can connect these low negative peaks with a "normalization constant" which is not particularly valuable for the comparison of these algorithms. However, higher positive peaks indicate clearly better focusing for point targets on edges when Range Stacking algorithm is applied (positive values here indicate this algorithm as a winner in focusing edge point targets because the Omega-k reconstructed image was subtracted from Range Stacking one).

Certainly, the drawback of the Range Stacking algorithm is its computational complexity. The processing of the SAS signal in Figure 5A by means of Matlab was almost 22 times longer than the Omega-k reconstruction. However, the unique feature of the Range Stacking algorithm allows to run the processing of each line $f(x,r_k)$ at the same time and thus significantly to accelerate the reconstruction step [2].

Applying a spatial filtering to the raw SAS signals with the use of Polar Format Processing did not have a significant influence on the comparison results. In this case, calculating some parameters was a little bit ambiguous because of appearing small distortions in a few point spread functions. However, almost identical distortions occurred in both Omega-k and Range Stacking reconstructed images. Therefore, it was not taken into account in the comparison process.

BIBLIOGRAPHY

- [1] Cumming I., Wong F., *Digital Processing of Synthetic Aperture Radar Data*, Artech House, Norwood 2005.
- [2] Soumekh M., *Synthetic Aperture Radar Signal Processing*, John Wiley & Sons, USA 1999.
- [3] Szczegielniak M., *Przetwarzanie Danych SAS Przy Pomocy Algorytmu Omega-K*, Proceedings of 52-th Open Seminar on Acoustics, pp. 111-114, Wągrowiec 2005.
- [4] Szczegielniak M., *Spatial SAS Signal Filtering by Means of Polar Format Processing*, Hydroacoustics, Vol. 9, pp. 191-198, 2005.

PORÓWNANIE ALGORYTMÓW OMEGA-K ORAZ RANGE STACKING W PRZETWARZANIU SAS

Streszczenie

Przetwarzanie SAS (Synthetic Aperture Sonar) jest wciąż rozwijane w kierunku lepszych, bardziej efektywnych oraz dokładnych algorytmów. Pożądane jest stosowanie algorytmów, które nie wprowadzają dodatkowych błędów z powodu aproksymacji fazy lub cyfrowej interpolacji danych. Jednym z takich algorytmów jest "Range Stacking". W artykule zaprezentowano jego krótką charakterystykę z wyróżnieniem jego wad i zalet w stosunku do innego, chętnie stosowanego algorytmu rekonstrukcji Omega-k. Wygenerowane sygnały SAS dla trybu "stripmap" zostały wykorzystane do praktycznego porównania obydwu algorytmów. Zbiór symulowanych obrazów SAS zawierał również sygnały przefiltrowane przestrzennie za pomocą algorytmu "Polar Format Processing". Wyniki numerycznych symulacji zostały zaprezentowane i przedyskutowane w artykule.

Słowa kluczowe: sonar z syntetyczną aperturą, range stacking, omega-k, porównanie